

Supplemental Materials

Molecular Biology of the Cell

de la Fuente-Ortega et al.

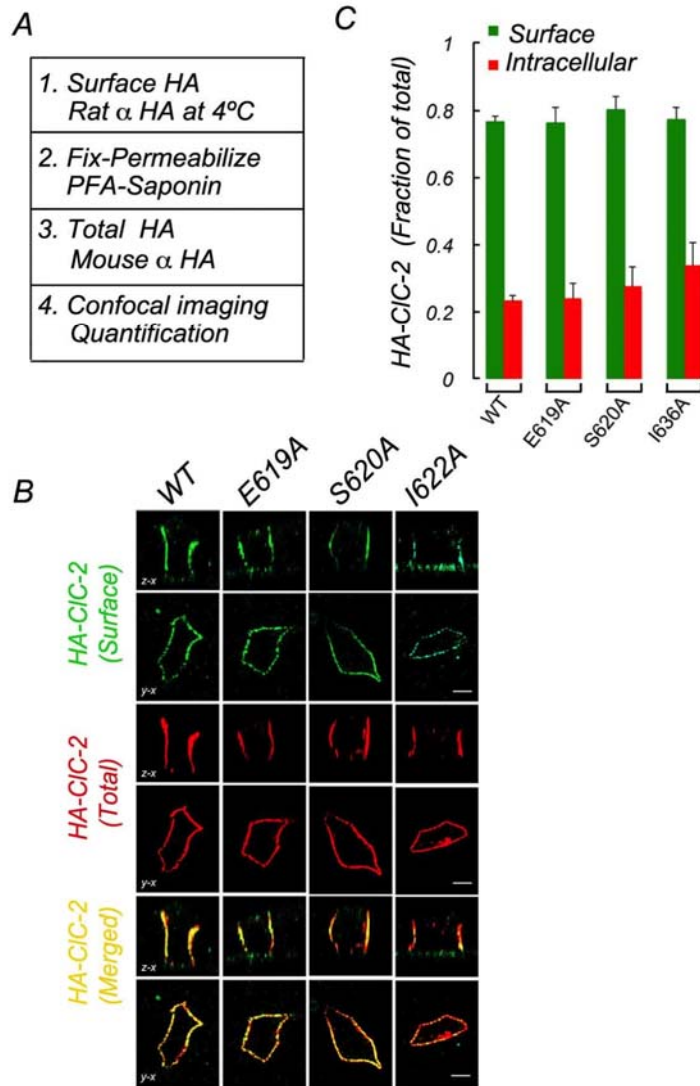
Supplemental Table S1: Surface distribution of HA-CIC-2 mutants in MDCK cells (statistical analysis of data corresponding to Figure 3).

HA-CIC-2	N	Surface			Intracellular		
		Mean	STDEV	SEM	Mean	STDEV	SEM
WT	6	0.795	0.076	0.031	0.205	0.076	0.031
L623A	15	0.288	0.105	0.027	0.712	0.105	0.027
L624A	12	0.517	0.085	0.025	0.483	0.085	0.025
L635A	13	0.736	0.092	0.025	0.264	0.092	0.025
L636A	12	0.638	0.175	0.051	0.362	0.175	0.051

Pair	Bonferroni	
	Surface	Intracellular
L623A vs WT	1.84E-11	1.84E-11
L624A vs WT	1.16E-04	1.16E-04
L624A vs L623A	4.12E-05	4.12E-05
L635A vs WT	1	1
L635A vs L623A	3.22E-13	3.22E-13
L635A vs L624A	1.54E-04	1.54E-04
L636A vs WT	0.08462	0.08462
L636A vs L623A	1.91E-09	1.91E-09
L636A vs L624A	0.12682	0.12682
L636A vs L635A	0.38061	0.38061
ANOVA	1.13E-14	1.13E-14

Data obtained from N regions of interest (ROI) from experiments as shown in figure 3 were analyzed with Origin9.1 statistical software using one-way ANOVA and further analyzed for multiple hypothesis testing using Bonferroni's correction. Numbers in red font represent statistically significant results.

Supplemental Figure S2: Sorting role of ESMI⁶²³LL non-leucineresidues.



Mutants of HA-CIC-2 with single-residue replacement of non leucine residues in the ESMI⁶²³LL motif were transiently expressed in MDCK cells and analyzed after 4 days in culture.

A) Scheme of sequential immunolabeling of HA-CIC-2 detected with mouse and rat antibodies to its luminal HA-epitope, before and after permeabilization, respectively (See “Materials and Methods” for details).

B) Surface (green) and total (red) immunolabeling of HA-CIC-2 in fully polarized cells. Note that alanine mutagenesis of ⁶¹⁹E, ⁶²⁰S and ⁶²²I did not affect the basolateral distribution of HA-CIC-2.

C) Bars represent surface and intracellular fractions of HA-CIC-2, calculated from confocal images (see Material and Methods for details). No statistical difference was observed in any of the residues mutated. Detailed statistical analysis is shown in supplemental Table S3.

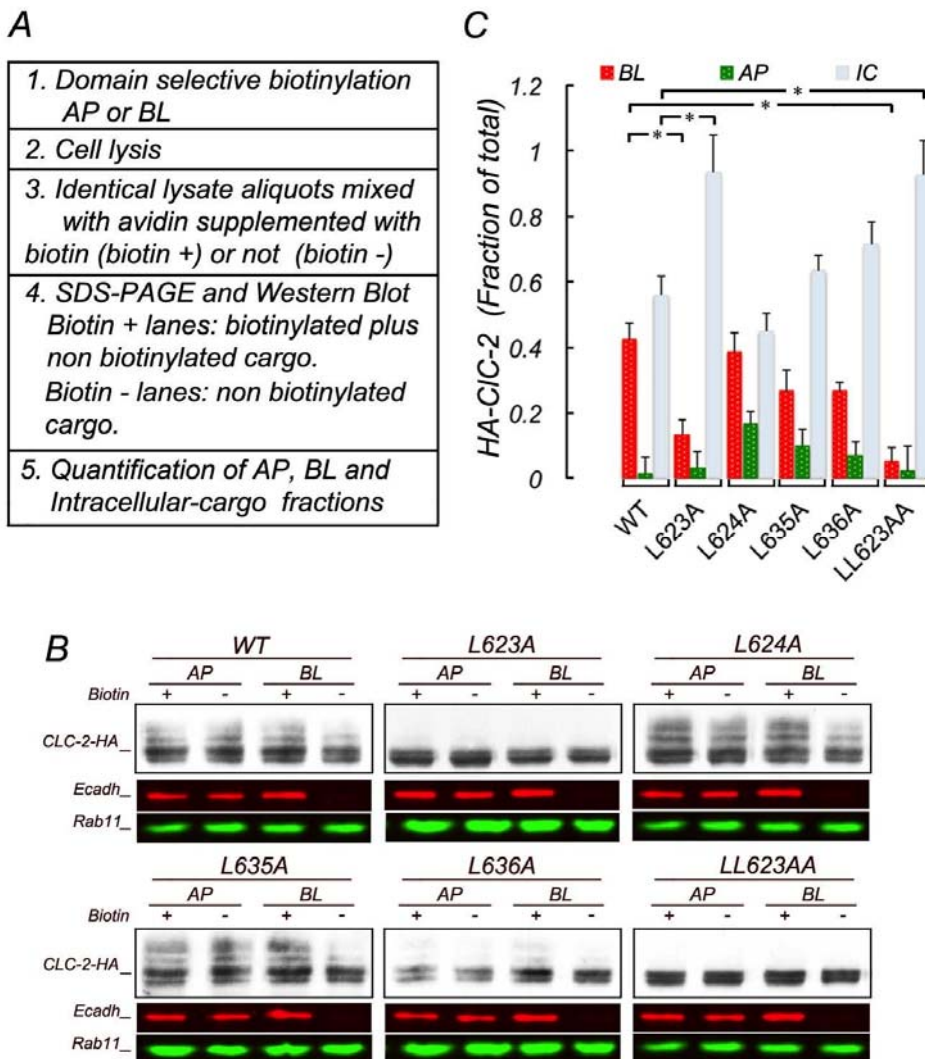
Supplemental Table S3: Surface and intracellular distribution of WT and mutant HA-CIC-2 with alanine substitutions in ESMILL (statistical analysis of data in Supplemental Figure S2).

<i>HA-CIC-2</i>	<i>N</i>	<i>Surface</i>		<i>Intracellular</i>	
		<i>Mean</i>	<i>SEM</i>	<i>Mean</i>	<i>SEM</i>
<i>WT</i>	6	0.76561	0.0176	0.23439	0.0176
<i>E619A</i>	9	0.76105	0.04615	0.23895	0.04615
<i>S620A</i>	8	0.80269	0.03823	0.27438	0.06159
<i>I622A</i>	8	0.77276	0.03707	0.33743	0.0684

<i>Pair</i>	<i>Bonferroni Test</i>	
	<i>Surface</i>	<i>Intracellular</i>
<i>E619A vs WT</i>	1	1
<i>S620A vs WT</i>	1	1
<i>S620A vs E619A</i>	1	1
<i>I622A vs WT</i>	1	1
<i>I622A vs E619A</i>	1	1
<i>I622A vs S620A</i>	1	1
<i>ANOVA</i>	0.23624	0.743

Data obtained from N regions of interest (ROI) from experiments as shown in supplementary Figure S2 were analyzed with Origin9.1 statistical software using one-way ANOVA and further analyzed for multiple hypothesis testing using Bonferroni's correction. No statistically significant results were observed.

Supplemental Figure S4: Trafficking roles of leucine residues in ESMI⁶²³LL and QVVA⁶³⁵LL using a biochemical assay.



A panel of lentiviruses encoding full length CIC-2 with single leucine to alanine substitutions in ESMI⁶²³LL and QVVA⁶³⁵LL was used to study the basolateral sorting signal role of these dileucine motifs.

- A)** Protocol used to quantify steady state apical (AP), basolateral (BL) and intracellular (IC) fractions of various mutants of HA-CIC-2 in polarized MDCK cells using a SBAS assay. Briefly, MDCK cells expressing WT or mutant HA-CIC-2, transduced via lentiviruses, are biotinylated from the apical or basolateral sides and lysed. The lysates are incubated with avidin in the absence (biotin -) or presence (biotin +) of biotin. The apical and basolateral fractions of WT and mutant HA-CIC-2 are calculated from the difference in band intensities between biotin + and biotin - samples, according to the equation $[(\text{biotin } +) - (\text{biotin } -)] / (\text{biotin } +)$.

- B)** Western blot of WT and mutant HA-CIC-2 processed as described in A. E-cadherin is shown as a positive control: its reduction in the BL biotin - lanes reflects its normal basolateral surface localization. Rab-11, a cytoplasmic protein, is shown as a negative control; as expected, no differences between biotin(+) and biotin(-) lanes were observed, reflecting its intracellular distribution.
- C)** Bars represent AP, BL and IC fractions of WT and mutant HA-CIC-2, calculated from western blot data derived from seven independent experiments (see statistical analysis in supplemental Table S5). Consistently with the quantitative immunolabeling assay shown in Figure 3, the data indicate that WT HA-CIC-2 [WT] is expressed predominantly on the basolateral PM with similar sizes of surface and intracellular pools. In contrast, HA-CIC-2[⁶²³L/A] and the double mutant HA-CIC-2[⁶²³LL/AA] show a dramatic reduction in the surface pool and increase in the intracellular pool. The differences observed with the other mutants were not statistically significant. These biochemical experiments, together with the quantitative immunolocalization experiments in Fig. 3 support the conclusion that ESMI⁶²³LL is the authentic basolateral sorting signal of CIC-2.

Statistical analysis is shown in supplemental Table S5

Supplemental Table S5: Surface distribution of HA-CIC-2 mutants in MDCK cells (statistical analysis of data corresponding to Supplemental Figure S4).

APICAL HA-CIC- 2	BASOLATERAL		INTRACELLULAR				
	N	Mean	SEM	Mean	SEM	Mean	SEM
WT	7	0.015	0.046	0.425	0.045	0.561	0.054
L623A	7	0.033	0.046	0.134	0.040	0.935	0.103
L624A	7	0.165	0.036	0.386	0.054	0.450	0.051
L635A	7	0.099	0.046	0.268	0.060	0.633	0.046
L635A	7	0.099	0.046	0.270	0.038	0.714	0.063
LL623AA	7	0.022	0.070	0.051	0.041	0.927	0.094

Bonferroni

Pair	AP	BL	IC
L623A WT	1	0.0015	0.01114
L624A WT	0.56223	1	1
L624A L623A	0.98772	0.00835	4.41E-04
L635A WT	1	0.35715	1
L635A L623A	1	0.77275	0.07826
L635A L624A	1	1	1
L636A WT	1	0.38183	1
L636A L623A	1	0.72647	0.53864
L636A L624A	1	1	0.20163
L636A L635A	1	1	1
LL623AA WT	1	3.24E-05	0.014
LL623AA L623A	1	1	1
LL623AA L624A	0.70997	1.96E-04	5.64E-04
LL623AA L635A	1	0.03543	0.09648
LL623AA L636A	1	0.03276	0.64365
ANOVA	2.36E-01	9.33E-06	6.55E-05

Data for statistical analysis were obtained from two independent experiments (one triplicate, one quadruplicate, N=7) and analyzed with Origin9.1 statistical software using one-way ANOVA; the data were further analyzed for multiple hypothesis testing using Bonferroni's correction. Numbers in red font represent statistically significant results

Supplemental Table S6: Intracellular distribution of HA-CIC-2 mutants in MDCK cells (statistical analysis).

HA-CIC-2	N	RE			TGN		
		Mean	STDEV	SEM	Mean	STDEV	SEM
WT	15	0.3127	0.1281	0.0331	0.0528	0.0369	0.0095
L623A	22	0.3152	0.0909	0.0194	0.1334	0.0829	0.0177
L624A	13	0.3638	0.1198	0.0332	0.0472	0.0264	0.0073
L635A	6	0.2795	0.1058	0.0432	0.0538	0.0438	0.0179
L636A	3	0.2510	0.0031	0.0018	0.0345	0.0199	0.0115

Bonferroni

Pair	RE	TGN
L623A vs WT	1	0.00121
L624A vs WT	1	1
L635A vs WT	1	1
L636A vs WT	1	1
L624A vs L623A	1	8.61E-04
L635A vs L623A	1	0.04349
L636A vs L623A	1	0.07743
L635A vs L624A	1	1
L636A vs L624A	1	1
L636A vs L635A	1	1
ANOVA	0.3793	9.19E-05

Wild type and mutants of HA-CLC-2 made by alanine substitution of single leucine in ESMI⁶²³LL or QVVA⁶³⁵LL motifs, were transiently expressed in MDCK cells.

Steady state distribution of HA-CIC-2 within TGN or recycling compartment (RE) was determined by confocal immunofluorescence after permeabilization with a rat anti-HA in combination with either rabbit or mouse antibodies to TGN38 or TfR, respectively. The extent of HA-CIC-2 co-localization values, expressed as the fraction of total HA-CIC-2 co-localizing with TGN38 or TfR were analyzed by one-way ANOVA to obtain mean, standard deviation, and p values obtained were subjected to multiple hypothesis testing using Bonferroni's (see statistical analyses in Material and Methods). A statistically significant increase in the TGN pool was found for HA-CIC-2^[623L/A] but not for other mutants. The recycling endosome (RE) pools of HA-CIC-2 [WT] and other mutants of CIC2-HA were not significantly changed.

Supplemental Table S7. Surface distribution of HA-CIC-2 in MDCK cells knocked-down for clathrin adaptors (statistical analysis of data corresponding to figure 4).

Surface <i>HA-CIC-2</i>	<i>N</i>	<i>Intracellular</i>					
		<i>Mean</i>	<i>STDEV</i>	<i>SEM</i>	<i>Mean</i>	<i>STDEV</i>	<i>SEM</i>
<i>WT</i>	8	0.588	0.115	0.041	0.412	0.115	0.041
<i>A-KD</i>	8	0.530	0.074	0.026	0.470	0.074	0.026
<i>B-KD</i>	8	0.501	0.135	0.048	0.499	0.135	0.048
<i>AB-KD</i>	11	0.287	0.112	0.034	0.713	0.112	0.034

Bonferroni

<i>Pair</i>	<i>Surface</i>	<i>Intracellular</i>
<i>A-KD WT</i>	1	1
<i>B-KD WT</i>	0.782329	0.782329
<i>B-KD A-KD</i>	1	1
<i>AB-KD WT</i>	1.24E-05	1.24E-05
<i>AB-KD A-KD</i>	3.02E-04	3.02E-04
<i>AB-KD B-KD</i>	1.46E-03	1.46E-03
<i>ANOVA</i>	6.85E-06	6.85E-06

Data obtained from N regions of interest (ROI) from experiments as shown in Figure 4 were analyzed with Origin9.1 statistical software using one-way ANOVA and further analyzed for multiple hypothesis testing using Bonferroni's correction. Statistically significant results are shown in red font.

Supplemental Table 8: Surface distribution of p75-CIC-2ct in clathrin adaptor knock down MDCK cells (statistical analysis of data corresponding to figure 5).

<i>p75-CIC-2ct</i>	<i>N</i>	<i>Apical</i>			<i>Basolateral</i>		
		<i>Mean</i>	<i>STDEV</i>	<i>SEM</i>	<i>Mean</i>	<i>STDEV</i>	<i>SEM</i>
<i>WT</i>	12	0.029	0.021	0.006	0.436	0.089	0.026
<i>A-KD</i>	8	0.023	0.015	0.005	0.528	0.078	0.028
<i>B-KD</i>	12	0.044	0.033	0.010	0.486	0.058	0.017
<i>AB-KD</i>	12	0.162	0.080	0.023	0.339	0.088	0.025

<i>Pair</i>	<i>Bonferroni</i>	
	<i>Apical</i>	<i>Basolateral</i>
<i>A-KD vs WT</i>	1	0.08936
<i>B-KD vs WT</i>	1	0.79695
<i>AB-KD vs WT</i>	1.37E-07	2.81E-02
<i>A-KD vs B-KD</i>	1	1
<i>A-KD vs AB-KD</i>	5.92E-07	3.46E-05
<i>B-KD vs AB-KD</i>	1.67E-06	3.13E-04
<i>ANOVA</i>	1.20E-08	1.93E-05

Data obtained from N regions of interest (ROI) from experiments as shown in Figure 5 were analyzed with Origin9.1 statistical software using one-way ANOVA and further analyzed for multiple hypothesis testing using Bonferroni's correction. Statistically s